Laser transmission welding of PEKK: Influence of material properties and process parameters on the weld strength

MATUS AGUIRRE Marcela[1,2,3,a] *, GARNIER Christian[1,b], GILBLAS Rémi[2,c],
COSSON Benoît[3,d], AKUÉ André[3,e], SCHMIDT Fabrice[2,f] and
CHABERT France[1,g]

[1]LGP-ENIT-INPT, 47 Avenue d'Azereix, Tarbes cedex BP1629-65016, France

[2]ICA-IMT Mines Albi, Campus Jarlard, 81013 Albi, CT Cedex 09, France

[3]IMT Nord Europe, Institut Mines Télécom, Univ. Lille, Centre Materials and Processes,
F-59653 Villeneuve d'Ascq, France

[a]mmatusag@enit.fr, [b]cgarnier@enit.fr, [c]rgilblas@mines-albi.fr,
[d]benoit.cosson@imt-nord-europe.fr, [e]andre.akue.asseko@imt-nord-europe.fr,
[f]fabrice.schmidt@mines-albi.fr, [g]fchabert@enit.fr

Keywords: Laser Welding, Thermoplastics, Optical Properties, Single Lap Shear Test

Abstract. Laser transmission welding (LTW) is a suitable process for assembling thermoplastic materials. This joining process is used to assemble most thermoplastics, but high-performance thermoplastics, such as polyetherketoneketone (PEKK), have received less attention until now. The present work deals with joining PEKK parts by LTW in amorphous over semi-crystalline state configuration. The optical properties of amorphous and semi-crystalline states were measured. The effect of the upper part thickness (2 or 4 mm) and those of the laser power reaching the interface was assessed through the determination of the heat affected zone (HAZ) dimensions and the mechanical resistance of the bonds. Single lap shear (SLS) tests were conducted to investigate the influence of the process parameters on the interfacial strength and to validate the weld quality. The highest LSS is obtained around 60 MPa. When increasing the laser power, the dimensions of the HAZ increase, and the mechanical strength decreases.

Introduction

Laser transmission welding (LTW) is an assembly process used for joining thermoplastic materials with a near-infrared (NIR) laser. Parts to be joined are overlapped and clamped together for welding. The laser beam faces the upper part and irradiates the assembly interface. Here, the laser energy is absorbed and converted into heat. This allows the polymers to melt at the interface and, by molecular interdiffusion, a weld seam is created during cooling.

For laser irradiation to reach the interface, the upper substrate needs to be transparent to the laser wavelength. To achieve the absorption at the interface, two techniques can be applied: use an absorbing medium at the joint interface; or assuring that the bottom substrate is absorbent at the wavelength of interest. For the first method, special NIR-absorbent dyes or pigments are applied at the joint interface, like ClearWeld® technology [1].

For the second one, a laser-absorbent part serves as lower substrate to achieve the energy absorption at the interface. However, most thermoplastics are transparent to the NIR laser radiation in their natural state. Although, the bottom substrate can be rendered absorbent by different methods. The first one is filling the polymer with an absorbing additive, like colorants [2,3] or reinforcements [4,5]. And the other and much less studied option is to increase the degree of crystallinity of the lower substrate to modify its optical properties. Indeed, the crystalline structure of semi-crystalline polymers limits the light transmission [6], and increases the light travel path,

leading to higher absorption [5,7], whereas an amorphous polymer is transparent in NIR. Despite its potential, this approach was rarely studied to weld thermoplastics.

High-performance thermoplastics such as Poly-Ether Ether Ketone (PEEK) and Poly-Ether Ketone Ketone (PEKK), can be processed into amorphous and crystalline states, depending on the processing conditions. Few works have studied LTW of PEEK and PEKK without additives. Amanat et al. studied the joining of PEEK films with ClearWeld® at the interface [8]. In their work, semi-crystalline PEKK assemblies showed a higher weld strength than amorphous PEEK joints, for all the laser speeds and power considered. Villar et al. welded PEKK thermo-compressed samples using an 808 nm NIR laser device [9]. They control the degree of crystallinity of PEKK to obtain quasi-amorphous and semi-crystalline samples, to be used as upper-transparent and lower-absorbent substrates, respectively. However, the results of mechanical strength of these welds are scarce in the literature, and none focus on PEKK welds.

In addition to the optical properties of the substrates, the process parameters can influence the bond quality in LTW: laser power, welding speed, laser beam size and, clamping pressure.

In this work, we study the joining process of amorphous and semi-crystalline PEKK by LTW. The optical properties and process parameters are correlated with the size and shape of the weld, as well as its mechanical strength. The originality is to keep constant the laser power reaching the interface while varying the thickness of the upper-substrate.

Materials and Methods

Kepstan® PEKK grade 7002 was supplied by Arkema France in pellets. PEKK 7002 is a semi-crystalline thermoplastic with tunable crystallinity due to its crystallization kinetics.

After drying the pellets at 120°C for 30 hours, specimens were manufactured by an injection molding press Proxima 50 from Billion. Two crystalline morphologies of unfiled PEKK were obtained: amorphous form (PEKK-A) and semi-crystalline form (PEKK-SC). Samples molded were plates of 95 × 95 mm² with 2 and 4 mm thick for amorphous form (PEKK-A2 and PEKK-A4 respectively), and 2 mm thick for PEKK-SC.

The molded plates were cut into 25 ± 3 mm width rectangular samples, then dried at 120°C for more than 24h and kept into a desiccator before welding. Acetone was used to clean the samples surfaces.

Differential Scanning Calorimetry (DSC) scans were carried out in a DSC 1 Stare System Mettler Toledo. Ramps of 10 K·min^{-1} were used for heating from 25°C to 380°C, and cooling from 380°C to 25°C. Glass transition temperature (Tg), melting temperature (Tm), cold crystallization temperature (Tcc) and degree of crystallinity (Xc) were obtained at heating. Cooling was used to obtain the crystallization temperature from melt (Tcm) and the maximum crystallinity (Xc-max).

The optical properties were measured using a FTIR spectrophotometer Bruker Vertex 70. Transmission (T) and reflection (R) factors were measured using an integration sphere with an Infragold Lambertian coating. Characterization was made at room temperature for the wavelength range of 0.9 to 2 µm. Absorption factors (A) are obtained using Eq. 1.

$$T + R + A = 1 \tag{1}$$

Transmissivity of clamping glass was experimentally measured using a power-meter Gentec Pronto-500, by comparing the output power measured before and after going through the glass.

Lap-joint configuration (Fig. 1) was used for welding, with an overlap of 12.5 mm, as indicated on ISO 4587:2003. The amorphous substrate was positioned over the semi-crystalline one.
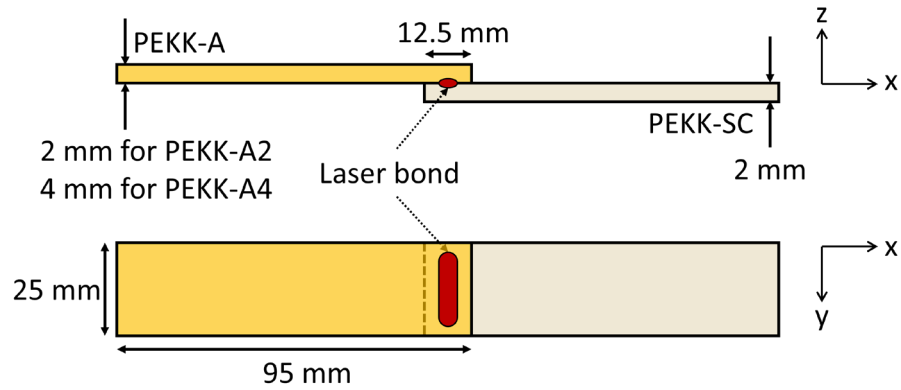
Fig. 1. Schematic diagram of lap-joint configuration used for welding PEKK-A/PEKK-SC (not to scale).

The assembly configuration is kept fixed on the welding machine platform. A support is placed under the amorphous sample to keep the interface parallel to the platform. A 15 mm thick semi-transparent glass plate is positioned over the assembly to apply the clamping pressure necessary to ensure intimate contact at the joint interface. The weld is created at the center of the overlap area using a moving laser. Thus, the interface is heated as the laser beam moves over the samples, following a predefined welding path. This LTW technique is known as *contour welding*.

Samples are welded using an ES weld 200 welding machine from ES Laser with a Diode laser of 975 nm. Output laser power can be set from 0 to 220 W with a resolution of ± 3 W. A circular shape laser beam is used with a beam diameter of 5 mm, obtained at maximum laser defocus. Clamping pressure is constantly applied at 3.8 MPa thanks to the glass plate. The welding path is a straight line: the laser beam moves from its initial position (L0) until the indicated weld length (Lw) of 20 mm, as shown in Fig. 2.

When a constant speed is used to irradiate the interface from L0 to Lw, an ovoidal weld bond is created instead of a thick line, as shown in Fig. 3A. To obtain a more homogeneous weld bond along the line laser path, like in Fig. 3B, a procedure combining static and dynamic irradiation is applied. The procedure starts by statically irradiating the interface for 2 seconds at L0. Then, the laser moves to irradiate at the given speed, from L0 to Lw. Finally, the laser statically irradiates the interface for 1 second at Lw. That allows to melt the interface all along the welding path in a more homogeneous shape of the weld bond (Fig. 3B).
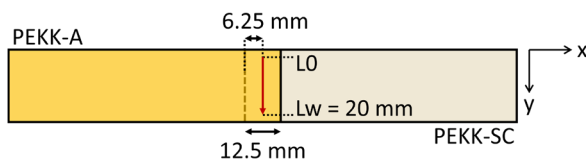

Fig. 2. Schematic diagram indicating the welding path position, direction and dimensions on the PEKK-A/PEKK-SC assembly.
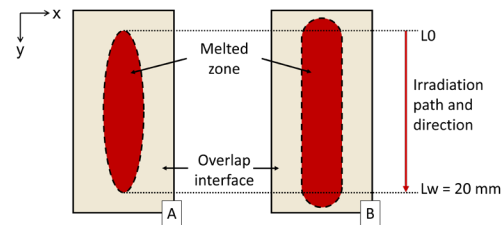

Fig. 3. Schematic diagram of the melted zone's shape created at the interface when irradiating with (A) dynamic condition, (B) static and dynamic condition.

The optimum welding speed to achieve the melting at the interface, regardless of the laser power, is 60 mm/min, as determined by previous tests. Thus, welding speed is kept constant for all welds. After irradiation, clamping pressure is maintained for 120 seconds while cooling.

Two process parameters are varied for this study: the transparent substrate thickness (2 and 4 mm) to obtain PEKK-A2/PEKK-SC and PEKK-A4/PEKK-SC assemblies, and the laser intensity. For the laser power, the preliminary welding tests indicated that the power-range needed at the interface to melt it without burning it is between 75 and 95 W. Thus, four power intensities were selected: 75, 85, 88, and 95 W. That provided eight configurations for the study (Table 1).

Table 1. Assembly configurations.

	75 W	85 W	88 W	95 W
PEKK-A2/PEKK-SC	A2/SC-P1	A2/SC-P2	A2/SC-P3	A2/SC-P4
PEKK-A4/PEKK-SC	A4/SC-P1	A4/SC-P2	A4/SC-P3	A4/SC-P4

Single lap shear (SLS) tests were carried out to characterize the lap-joint welded samples strength. An INSTRON 550R tensile machine was used with a load cell of 50kN and a cross head load rate of 2800 N·mm^{-1}. Each sample was tested until failure. The load at failure F_f [N] was recorded and the type of failure mode was identified. Also, the normalized lap-shear strength LSS [MPa] was obtained by dividing the force at failure by the contact area Ac [mm²]. This area was measured by microscopy for the samples that failed at the interface.

Visual inspection of the welds was carried out with a numerical optical microscopy VHX-6000S from Keyence. Post-failure bond interfaces were characterized to obtain the shape and dimensions of each weld. The weld cross-sections of post-welding bonds were visualized to characterize the HAZ along the weld path.

Results

Thermal transitions.

Fig. 4A shows a typical DSC thermogram of PEKK 7002 amorphous specimens. Tg is $158 \pm 2°C$ and Tm is measured at $317 \pm 2°C$. Crystallization temperatures are around $202 \pm 1°C$ for Tcc, and $295 \pm 1°C$ for Tcm.
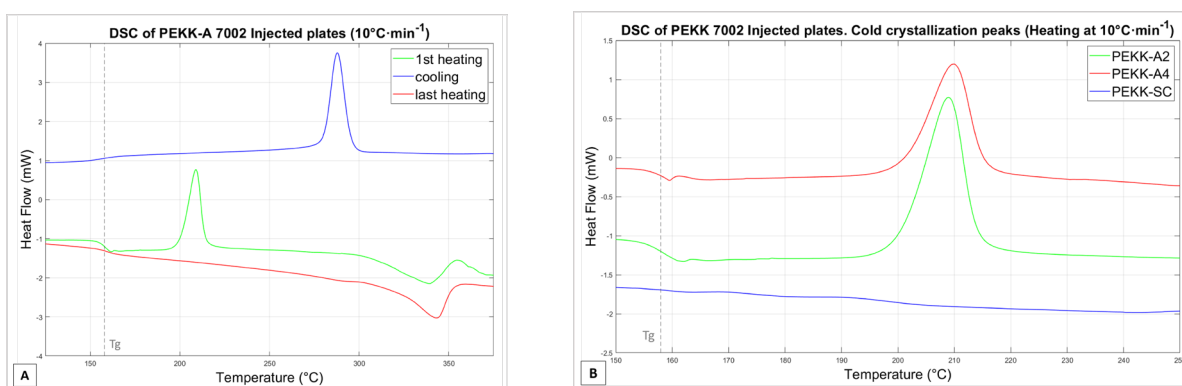

Fig. 4. (A) DSC scans of PEKK 7002 amorphous molded plates. (B) cold crystallization peaks of molded samples obtained on the first heating DSC scan.

In Fig. 4B, an exothermic peak is observed around 200°C for amorphous samples (green and red curves), after glass transition. This indicates cold crystallization, occurring when the sample is not fully crystallized. Indeed, right after Tg, the macromolecules have gained enough mobility to self-organize into crystalline structures. For PEKK-SC, no peak is observed because the sample is

already fully crystallized. To assess the degree of crystallinity, the enthalpy of this peak (ΔHcc) is subtracted from the melting enthalpy of the first heating (ΔHm), then the result is divided by the enthalpy of 100 % crystallized polymer ($\Delta H_{100\%}$), considered as same as PEEK (130 J·g^{-1}) [10]. A degree of crystallinity of $4 \pm 2\%$ was found for PEKK-A and $20 \pm 2\%$ for PEKK-SC.

Optical properties.

The laser irradiation that strokes the samples' surface can be transmitted, reflected and/or absorbed. For that, transmission, reflection and absorption factors of the samples need to be determined. The transmission factor (T) characterizes the quantity of incident laser irradiation that will be able to go through its thickness. The reflection factor (R) indicates the portion of the irradiation that will be reflected by the material surface. Finally, absorption factor (A) will provide the fraction of the incident irradiation that will be absorbed by the material, either at the surface or in the volume. These three factors are related between them by Eq. 1 and they can be expressed in percentage for the desired wavelength.

In the visible light spectral range, PEKK-A has a natural yellow translucent coloration, whereas PEKK-SC samples are opaque with a natural beige color. Their optical properties are necessary to verify their compatibility with LTW at 975 nm. The results are gathered in Table 2.

Table 2. Transmission, reflection and absorption factors of PEKK molded samples.

Substrate	T [%]	R [%]	A [%]
PEKK-A2	75 ± 1.5	13 ± 0.1	12 ± 0.1
PEKK-A4	62 ± 0.7	13 ± 0.1	25 ± 0.1
PEKK-SC	20 ± 0.02	48 ± 1.7	32 ± 1.7

The transmission spectrum of PEKK samples is seen in Fig. 5. At 975 nm, PEKK-A samples have a transmission factor higher than PEKK-SC ones: 75 % for PEKK-A2 and 62 % for PEKK-A4, against 20 % for PEKK-SC. Also, increasing the thickness of PEKK-A decreases the transmission factor by more than 17 %. Based on previous works of LTW on PEKK [9] a transmission factor of 60% is suitable to achieve melting at the interface. Consequently, 2 and 4 mm thick PEKK-A samples seem adequate to be used as transparent upper substrate for LTW.
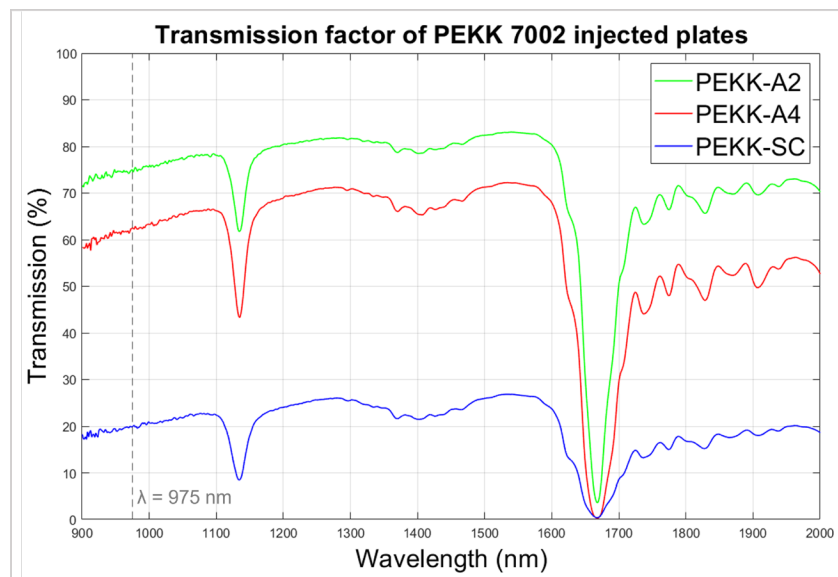

Fig. 5. Transmission spectrums of PEKK 7002 molded samples.

Table 2 pointed out that the sample with the highest absorption factor is the semi-crystalline one. Even if its absorption is low (32 %), it is higher than its transmission factor (20 %). This validates the suitability of PEKK-SC as absorbent substrate for LTW.

To irradiate the assembly interface, the output laser irradiation (Po) will first go through the clamping glass and then through the transparent substrate. Therefore, the output laser power value will decrease after going through each layer, according to the transmission factor of each layer. Hence, the power reaching the assembly interface will be the percentage of output power that the glass and the transparent substrate will allow to transmit. At our laser wavelength, the clamping glass has a transmissivity of 0.82, as evaluated with the power-meter. Then, the transmission factor of the transparent-upper substrate depends on its thickness: 0.75 for PEKK-A2, and 0.62 for PEKK-A4. Thus, the power at the interface (Pint) can be calculated using Eq.2 and Eq.3 for PEKK-A2/PEKK-SC and PEKK-A4/PEKK-SC, respectively.

$$P_{int(A2)} = P_0 \times 0.82 \times 0.75 \tag{2}$$

$$P_{int(A4)} = P_0 \times 0.82 \times 0.62 \tag{3}$$

The power at the interface is set between 75 and 95 W. Table 3 indicates the output laser power used for each type of assembly to obtain the desired power at the interface for each targeted power.

Weld characterization.

The cross-section of the weld bond along the weld path is observed to characterize its heat affected zone (HAZ).

Table 3. Laser power used for LTW.

	P_0 [W]		P_{int} [W]
	for A2/SC	for A4/SC	For both
P1	123	148	75
P2	139	168	85
P3	144	175	88
P4	154	188	95

Fig. 6 shows a micrograph of the assembly cross-section before and after welding for A4/SC-P2. Before welding, we can easily identify the interface line between the overlapped substrates (inside the red dashed rectangle in Fig. 6A). After welding, the HAZ appears as an oval shape replacing the interface line (inside the red dashed contour in Fig. 6B). The color change from yellow to white within the HAZ demonstrates a modification of the crystallinity. All the weld bonds characterized showed this same shape and aspect on their HAZ.

The PEKK-SC shows a yellow coloration within the HAZ: the substrate became amorphous on cooling. This means that PEKK-SC absorbed enough laser power to melt at the interface and that the cooling ramp was faster than the crystallization kinetics. Also, in PEKK-SC, the HAZ is so deep that it almost reaches the bottom of the substrate. It indicates that the laser irradiation penetrated the sample, as stands by Jones et al. [1], and was absorbed on the volume and not only at the interface. The average depth for both types of assemblies is 1.4 ± 0.2 mm. With these parameters, it would not be possible to weld lower parts thinner than 1.4 mm.

In PEKK-A substrate, the HAZ colors go from yellow to white. The melting zone is mainly located at the interface. The white color indicates that PEKK-A sample undergoes cold crystallization. Tcc was measured at 202°C in Fig.4. Following laser absorption at the interface, this temperature was achieved by heat conduction from the lower part. Moreover, the shape and colors of HAZ indicates that the samples really merged at the interface to create a strong bond.
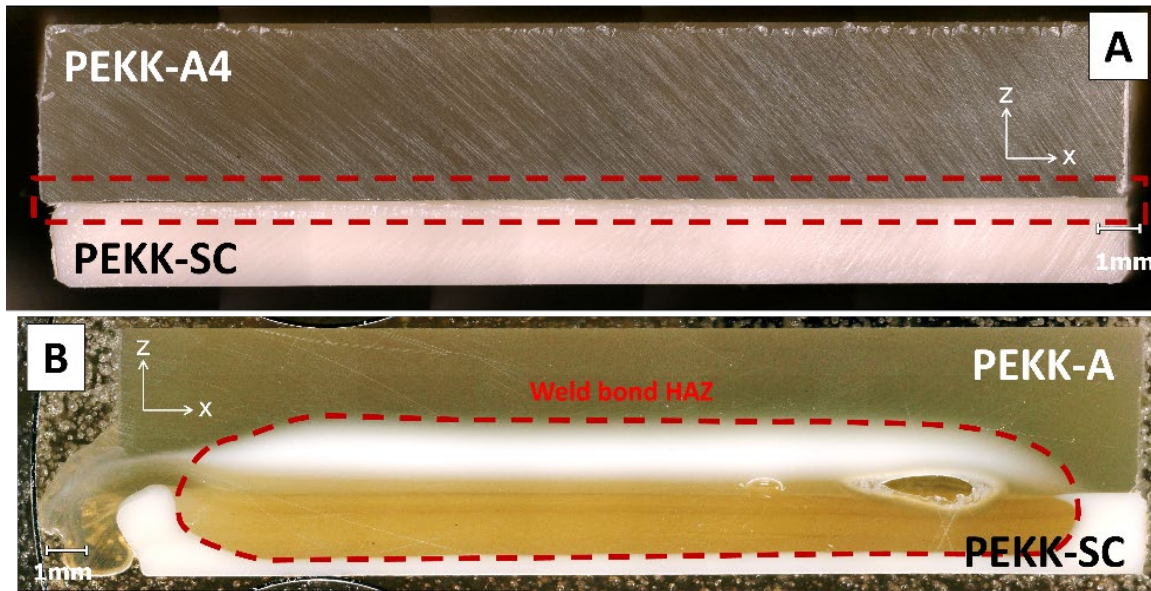
Fig. 6. A4/SC-P2 assembly cross-section along the welding path (A) before and (B) after welding.

HAZ dimensions were measured for each assembly configuration. Its height (along the X axis) and length (along the Z axis) were plotted against the power used for welding in Fig. 7. A notorious increment on the HAZ dimensions with the power is noticed. This increase is almost linear for three of the four intensities (75, 85 and 95 W). The HAZ dimensions obtained at 88 W do not follow the regular trend. A possible explanation is related to the uncertainty of the power. Indeed, the values of power are defined with ± 3%. Thus, the data obtained for 85 and 88 W are expected to be close to each other.

For the HAZ height, almost 1 mm of difference is found from lowest to highest power, for both types of assemblies (A2/SC and A4/SC). Concerning the length of the HAZ, it is quite the same on A4/SC, with only 0.3 mm of difference from the lowest to the highest power. For A2/SC, this length improves considerably with laser intensity, with a gap of 1.6 mm. Moreover, this HAZ length is higher than the welding path used for welding (20 mm) in all the configurations. That indicates that the irradiation procedure used, combining static and dynamic irradiation, had a positive impact on the melting at the interface. This increment of the HAZ dimensions with laser power can be explained by the fact that increasing the laser power maximizes the heat input which leads to a greater volume of melted material at the interface, resulting in a higher welded zone.

The HAZ dimensions also increase with the increase of the transparent substrate thickness for each laser power. This can be caused by the scattering of the laser irradiation through the samples. Thus, PEKK-A4 seems to scatter more the light than PEKK-A2, which increases the distribution of the energy over a larger area.
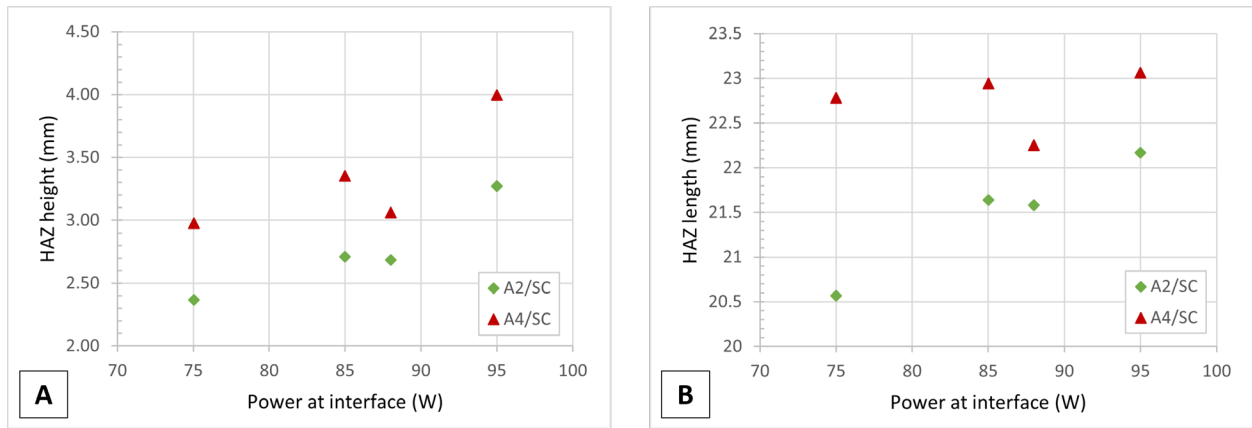
Fig. 7. HAZ dimensions (A) height and (B) length, plotted against the laser power used at the interface.

Different mechanical tests are carried out to quantify the resistance of welded samples by LTW: DCB [2,11], wedge [12], and SLS tests [8,11,13-16]. SLS is the easiest and most used test. When tested in SLS, lap-joint welded samples failed in different modes. To identify their failure type, four failure modes are defined (Table 4) inspired by the classification proposed by Amanat et al. [8] for LTW on PEEK. Two types of failure were obtained within our assemblies:

- *Cohesive failure*: this indicates that the bond broke and was separated as if it was ripped off. The samples actually fused at the interface, creating a strong weld.
- *Substrate near joint*: one or both substrates broke near the weld bond, but the bond was fully or mostly intact, proving that the bond strength is superior to the substrate strength.

Table 4. Failure modes for LTW samples tested by SLS.

Failure mode	Appearance	Inference	Description
Interfacial		Bond strength << substrate strength	Assembly fails at the interface because no real material cohesion was created at the irradiated interface. Most undesired result.
Cohesive		Bond strength ~ substrate strength	Assembly fails at the interface within the weld bond created.
Substrate near joint		Bond strength > substrate strength	Failure within the substrate but near the interfacial region and weld bond intact (or mostly).
Bulk substrate		Bond strength >> substrate strength	Bulk substrate results in tensile yield and brakes far from the weld bond. Most desired result.

Even though two failure modes were obtained, only the samples that failed in cohesive mode are analyzed in this paper. The overlap interface is visible so the real contact area can be measured to obtain the LSS value for each cohesively failed assembly. 1 or 3 samples over 5 failed cohesively for each configuration. A hypothesis steaming from this high dispersion is related to the irradiated surface that can vary locally due to heterogeneities of the samples: different macromolecular organization, and micro-voids or particles inside them. These heterogeneities can lead to the scattering of the laser path in the upper substrate, and to an inhomogeneous absorption of the laser irradiation in the bottom substrate. The LSS obtained are plotted with the power for both type of assembly in Fig. 8.
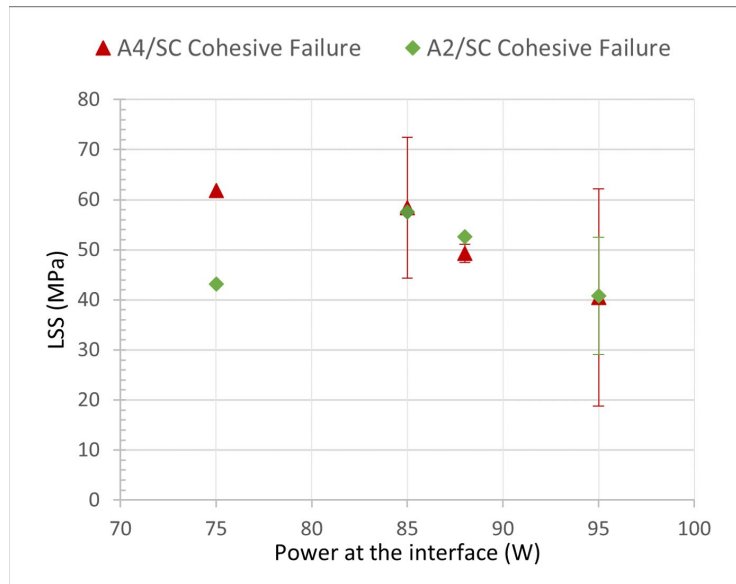
Fig. 8. LSS (MPa) of LTW samples failed cohesively. Bars indicate the measuring range.

The strength obtained at one laser power is the same for both types of assemblies except for the first laser power of 75 W. However, the strength decreases with laser power from 85 W. This drop in weld strength can be caused by different crystalline morphology at the interface. Indeed, the crystallinity of PAEK is strongly impacted by its thermal history. A higher power reaching the interface would result in a higher temperature and slower cooling ramp. As proved on PEEK [17], the refinement of the primary lattice takes place when the temperature is higher than or equal to the previous crystallization temperature. An evolution of the lattice sizes could result in lower ultimate tensile strength. Further studies are needed to clarify this point. Overall, the strength of our assemblies is higher than those achieved by Potente et al. when welding PEEK T-joint specimens with similar thicknesses for the transparent substrate [18]. They achieved a maximum strength of 40 MPa, while our minimum is of the same value for both types of assemblies.
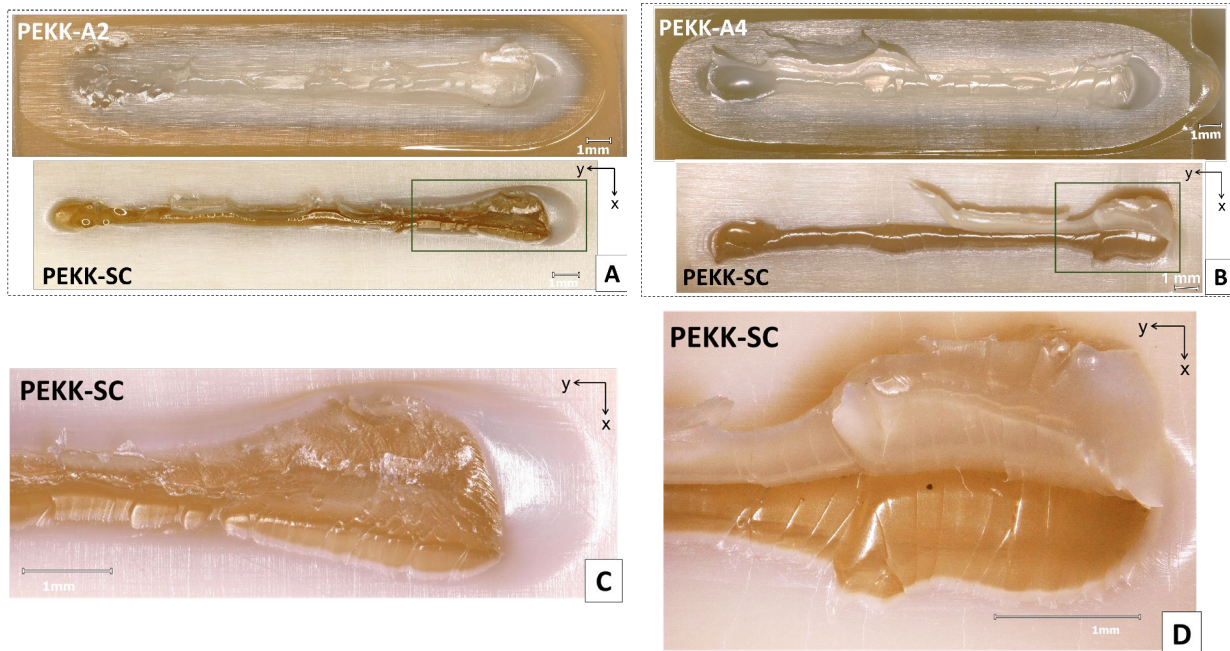
Fig. 9. Weld bond of assemblies failed with cohesive mode. The opened overlapped interfaces allow to visualize the weld bond on each substrate of the assembly for (A) A2/SC-P2 and (B) A4/SC-P2. (C) Magnified view of inset show in (A). (D) Magnified view of inset shown in (B).

The cohesively failed weld bonds were characterized by optical microscopy. Fig. 9 shows the micrograph of the opened overlap of cohesively failed assemblies in the PEKK-A and PEKK-SC substrates. The weld bonds show signs of sheared material on each substrate. That indicates that the samples were melted and fused together at the irradiated zone and that the bonds were shared during mechanical test.

Summary

PEKK 7002 grade is suitable to be welded with amorphous over semi-crystalline sample configuration. The following conclusions are outlined:

- The optical properties of the substrates were measured in injection molded plates:
  - A transmission factor of 40 % is measured on amorphous plates at the wavelength of interest, even with 4 mm thick. Thus, the amorphous state is transparent enough to allow LTW.
  - Increasing the thickness of the amorphous substrate from 2 to 4 mm decreases the IR transmission factor by 17 %.
  - The absorption properties of the semi-crystalline state of PEKK 7002 make it suitable for LTW.
- We targeted to define the process parameters according to the material properties to get a strong and reliable weld.
  - The output laser power was varied to obtain the same laser intensity radiation at the interface considering the transmission factor of the transparent substrate.
  - The welding speed and irradiation procedure were established to allow the materials to melt at the interface all along the welding path.
- Relationships between the process parameters, the material properties and the dimensions of the HAZ, and the mechanical resistance of the welds were determined. The highest LSS

is 60 MPa, demonstrating the ability of LTW in achieving strong welds in amorphous over semi-crystalline PEKK.

Further work will focus on extending the study to other process parameters. A thorough characterization of the HAZ will be carried out to link the crystalline morphology to the thermal history undergone within the HAZ.

References

[1] I. Jones, Laser welding for plastic components, Assem. Autom. 22 (2002) 129-135. https://doi.org/10.1108/01445150210697429

[2] F. Chabert, C. Garnier, J. Sangleboeuf, A.C.A. Asseko, B. Cosson, Transmission Laser Welding of Polyamides: Effect of Process Parameter and Material Properties on the Weld Strength, Procedia Manuf. 47 (2020) 962-968.

[3] N. Amanat, C. Chaminade, J. Grace, N. James, D.R. Mckenzie, Optimal process parameters for thermoplastic polyetheretherketone joints fabricated using transmission laser welding and Lumogen® IR absorptive pigment, J. Laser. Appl. 23 (2011) 012003. http://doi.org/10.2351/1.3552972

[4] S. Berger, F. Oefele, M. Schmidt, Laser transmission welding of carbon fiber reinforced thermoplastic using filler material—A fundamental study, J. Laser. Appl. 27 (2015) S29009. https://doi.org/10.2351/1.4906391

[5] X.F. Xu, A. Parkinson, P.J. Bates, G. Zak, Effect of part thickness, glass fiber and crystallinity on light scattering during laser transmission welding of thermoplastics, Opt. Laser. Technol. 75 (2015) 123-131. https://doi.org/10.1016/j.optlastec.2015.06.026

[6] V. Kagan, R.G. Bray, Advantages and limitations of laser welding technology for semi-crystalline reinforced plastics, Int. Congr. Appl. Lasers Electro-Opt, Jacksonville, Florida, USA, Laser Institute of America, 2001 [cited 2022 Dec 11], 1218-1227. Available from: http://aip.scitation.org/doi/abs/10.2351/1.5059784

[7] V.A. Kagan, R.G. Bray, W.P. Kuhn, Laser Transmission Welding of Semi-Crystalline Thermoplastics—Part I: Optical Characterization of Nylon Based Plastics, J. Reinf. Plast. Compos. 21 (2002) 1101-1122. https://doi.org/10.1177/073168402128987699

[8] N. Amanat, C. Chaminade, J. Grace, D.R. Mckenzie, N. James, Transmission laser welding of amorphous and semi-crystalline poly-ether-ether-ketone for applications in the medical device industry, Mater. Des. 31 (2010) 4823-4830. http://doi.org/10.1016/j.matdes.2010.04.051

[9] M. Villar, C. Garnier, F. Chabert, V. Nassiet, D. Samelor, J.C. Diez, A. Sotelo, M.A. Madre, In-situ infrared thermography measurements to master transmission laser welding process parameters of PEKK, Opt. Laser. Eng. 106 (2018) 94-104. https://doi.org/10.1016/j.optlaseng.2018.02.016

[10] T. Choupin, L. Debertrand, B. Fayolle, G. Regnier, C. Paris, J. Cinquin, B. Brule, Influence of thermal history on the mechanical properties of poly(ether ketone ketone) copolymers, Polym. Cryst. 2 (2019) e10086. https://doi.org/10.1002/pcr2.10086

[11] T.B. Juhl, J. de C. Christiansen, E.A. Jensen, Mechanical testing of polystyrene/polystyrene laser welds, Polym. Test. 32 (2013) 475-481. http://doi.org/10.1016/j.polymertesting.2013.01.009

[12] M.A. Villar montoya, Procédé de soudage laser de polymères haute performance : établissement des relations entre les paramètres du procédé, la structure et la morphologie du polymère et les propriétés mécaniques de l'assemblage, PhD Thesis, Toulouse, INPT, 2018. Available from: http://www.theses.fr/2018INPT0118

[13] A. Korycki, C. Garnier, M. Bonmatin, E. Laurent, F. Chabert, Assembling of Carbon Fibre/PEEK Composites: Comparison of Ultrasonic, Induction, and Transmission Laser Welding, Materials 15 (2022) 6365. https://doi.org/10.3390/ma15186365

[14] T.B. Juhl, J. de Claville Christiansen, EA. Jensen, Investigation on high strength laser welds of polypropylene and high-density polyethylene, J. Appl. Polym. Sci. 129 (2013) 2679-2685. https://doi.org/10.1002/app.39000

[15] V. Wippo, Y. Winter, P. Jaeschke, O. Suttman, L. Overmeyer, The Influence of Laser Welding Processes on the Weld Seam Quality of Thermoplastic Composites with High Moisture Content, Phys. Procedia 83 (2016) 1064-1072. https://doi.org/10.1016/j.phpro.2016.08.112

[16] A.C. Akué Asséko, B. Cosson, É. Lafranche, F. Schmidt, Y. Le Maoult, Effect of the developed temperature field on the molecular interdiffusion at the interface in infrared welding of polycarbonate composites, Compos. Part B Eng. 97 (2016) 53-61. https://doi.org/10.1016/j.compositesb.2016.04.064

[17] L. Martineau, F. Chabert, B. Boniface, G. Bernhart, Effect of interfacial crystalline growth on autohesion of PEEK, Int. J. Adhes. Adhes. 89 (2019) 82-87. https://doi.org/10.1016/j.ijadhadh.2018.11.013

[18] H. Potente, F. Becker, G. Fiegler, Investigations towards application of a new technique on laser transmission welding, Weld World. 45 (2001) 15-20.